Bioprocess Biosyst Eng (2010) 33:971–978
DOI 10.1007/s00449-010-0421-y

ORIGINAL PAPER

# Electrochemical recognition for sugars on the chitosan-poly(diallyldimethylammonium chloride)-nano-Prussian blue/nano-Au/4-mercaptophenylboronic acid modified glassy carbon electrode

**Xiu Zhu Bian · Hong Qun Luo · Nian Bing Li**

Received: 27 December 2009 / Accepted: 18 March 2010 / Published online: 6 April 2010


**Abstract** A new amperometric biosensor for the detection of sugars was prepared. A glassy carbon electrode was modified with Prussian blue (PB) nanoparticles protected by chitosan (CS) and poly(diallyldimethylammonium chloride) (PDDA), and then gold nanoparticles were assembled onto the electrode followed by the assembly of 4-mercaptophenylboronic acid (MPBA) onto the surface of gold nanoparticles through a sulfur–Au bond to fabricate a self-assembled biosensor. The PB nanoparticles protected by CS and PDDA were characterized using transmission electron microscopy and UV–vis absorption spectroscopy. The characterization of the self-assembled electrode was investigated by cyclic voltammetry and electrochemical impedance spectroscopy. The p$K_a$ values of the MPBA monolayer before and after combining with sugars were determined. The fabricated electrode exhibited excellent performances for determining D(+)-glucose, D(+)-mannose, and D(−)-fructose on the basis of the change in $i_p$ of the $Fe(CN)_6^{3-/4-}$ ion in the presence of sugars.

**Keywords** Gold nanoparticles · Nano-Prussian blue · 4-Mercaptophenylboronic acid · Sugars · Biosensor

## Introduction

In recent years, too much attention has been paid to inorganic nanoparticles like gold [1], silver [2], and platinum metals [3] because of their significant properties like the high surface areas, strong adsorption ability, and a heterogeneous electron transfer catalyzing ability [4]. Prussian blue (PB) is one of the longest described coordination compounds, which has been extensively studied in basic and technologically oriented research and has been found a new range of interesting applications [5], such as electrochemical [6], photophysical [7], electrochromic [8, 9], and magnetic properties [10], and potential analytical applications [11–14]. Due to its excellent electrocatalysis, PB has been widely used as an electron transfer mediator in the amperometric biosensors [15–17]. For example, the PB modifier strongly catalyzes the reduction of hydrogen peroxide in a negative operating potential range, which offers the most sensitive and interference-free detection [18].

However, the traditional and common method for the preparation of PB modified electrodes is based on the electrodeposited PB film, which usually shows intrinsic shortcomings of instability for leaking [19]. To solve this problem, a large number of PB nanoparticles have been synthesized with the stabilizers, such as poly (vinylpyrrolidone) (PVP) [20, 21], chitosan (CS) [22], poly(diallyldimethylammonium chloride) (PDDA) [20, 23, 24], polyallylamine hydrochloride (PAH), polystyrene sulfonate (PSS), and polyvinyl alcohol (PVA) [25]. These protective polymers could not only control the growth and handle the agglomeration of nanoparticles, but also bring attractive novel properties to the nanoparticles, such as biocompatibility, solubility and film-forming properties [26]. Due to these attractive properties of PB nanoparticles protected by organic polymers, the application of PB is broadened in biosensors.

Sugars are important energy substances and have been widely applied in the food industry and medicine. Fast and

X. Z. Bian · H. Q. Luo · N. B. Li (✉)
Education Ministry Key Laboratory on Luminescence and Real-Time Analysis, School of Chemistry and Chemical Engineering, Southwest University, Chongqing 400715, People's Republic of China
e-mail: linb@swu.edu.cn

accurate determination of sugars has therefore attracted much attention of the researchers. Up to now, many efforts have been contributed to the development of techniques for the determination of sugars based on the electrochemical method [27], chemiluminescence [28], chromatography [29], capillary electrophoresis [30], and the enzymatic method [31]. Each method has itself advantages. However, there has been increasing interest in the development of a new detection method in the recent decade. Boronic acid and its derivatives as recognition molecules for sugars have become the focus. They can form reversible bonds with 1,2- or 1,3-diols of sugars to generate five- or six-membered cyclic complexes [32]. Therefore, the boronic acid derivatives can be immobilized on the surface for the transducers such as electrodes to detect sugars.

In the present work, a new biosensor has been fabricated using self-assembly technique. The surface of glassy carbon (GC) electrode was modified with PB nanoparticles protected by chitosan (CS) and PDDA and then colloidal Au was assembled onto the modified surface. Following this, MPBA was immobilized to the electrode surface easily through a sulfur–Au bond. The fabricated electrode exhibited excellent performances for determining glucose, mannose, and fructose. Based on this phenomenon, a new biosensor for the determination of sugars was developed.

## Experimental section

### Reagents

D-Glucose and chitosan (CS) were purchased from Sigma. D-mannose and D-fructose were purchased from Fluka. Poly(diallyldimethylammonium chloride (PDDA, Mw: 200,000—350,000 g/mol, 20 wt% in water) and 4-mercaptophenylboronic acid (MPBA) were purchased from Aldrich. Gold chloride tetrahydrate was purchased from Shenyang Research Institute of Nonferrous Metals. All other reagents were of analytical grade and were used without further purification. Phosphate buffer solutions (PBS) with various pH values were prepared with 0.1 M $NaH_2PO_4$, 0.1 M $Na_2HPO_4$, and a small amount of 0.1 M HCl or NaOH. Doubly distilled water was used throughout.

### Apparatus

A CHI 660B electrochemical workstation (CH Instruments, USA) was used for the measurement of cyclic voltammetry (CV) and electrochemical impedance spectra (EIS). A three-electrode system used in the measurements consists of a GC or modified GC electrode as the working electrode, platinum wire as the counter electrode, and a saturated calomel electrode (SCE) as the reference electrode. Transmission electron microscopy (TEM) images were recorded with a H7500 (Hitachi Co., Japan). A UV-vis 8500 spectrophotometer (Tianmei Co., Shanghai, China) was used for measuring absorption spectra. A pHS-3D pH meter (Shanghai Analytical Instrument Factory, Shanghai, China) was used for pH measurement.

### Synthesis of PB nanoparticles protected by CS and PDDA

PB nanoparticles protected by CS and PDDA were synthesized according to the literature [26] but with a slight modification. Briefly, 8.0 mL of 6.25 mM $FeCl_3$ (containing 0.4% PDDA, v/v) and 8.0 mL of 0.15 wt% CS solution were mixed under vigorous stirring and then 2.0 mL of 25 mM $K_4[Fe(CN)_6]$ solution was slowly dropped into the mixed solution under vigorous stirring at room temperature. When the solution color changed gradually to dark blue, PB nanoparticles were formed, and the resulting dark blue colloidal solution was used as a CS–PDDA–nano-PB stock solution.

### Preparation of colloidal gold

Au colloids were prepared according to Frens [33] with slight modifications. First, 1.0 mL of 1% $HAuCl_4$ was brought to 100 mL of boiling doubly distilled water with vigorous stirring in a 250 mL round-bottom flask. Then, 2.5 mL of 1% sodium citrate was added to the vortex of the solution quickly, which resulted in a color change from pale yellow to dark red. Boiling was continued for 10 min, the heating mantle was then removed, and stirring was continued until the solution reached room temperature.

### Fabrication of the modified electrode

A glassy carbon electrode ($\Phi = 3$ mm) was polished to a mirror using 0.3 and 0.05 μm alumina slurry followed by rinsing thoroughly with doubly distilled water. After being sonicated successively in 1:1 nitric acid and doubly distilled water, the electrode was allowed to dry at room temperature. The cleaned electrode was modified with CS–PDDA–PB nanoparticles by a simple casting method. Typically, 7.5 μL of CS–PDDA–nano-PB solution was cast on the electrode surface and the electrode was allowed to dry at room temperature to obtain a GC/CS–PDDA–nano-PB modified electrode. After the modified electrode was thoroughly rinsed with water, it was immersed in 2.0 mL of prepared gold colloids for 9 h to form a nano-Au monolayer. Then the electrode was placed into 4-mercaptophenylboronic acid solution (0.5 mg/mL in tetrahydrofuran–methanol = 9:1, v/v) for approximately 10 h to obtain the final self-assembled electrode. The fabrication

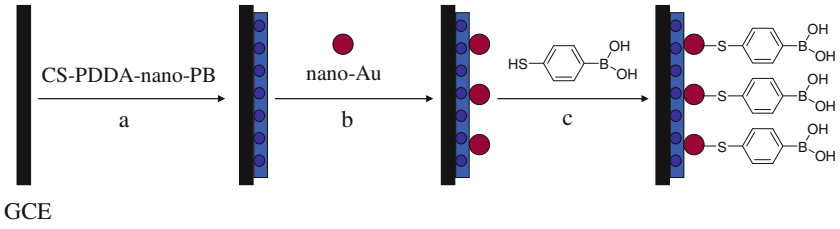


**Scheme 1** Schematic illustration of the stepwise self-assembly fabrication process: **a** formation of CS-PDDA-nano-PB layer, **b** formation of nano-Au monolayer, **c** MPBA loading

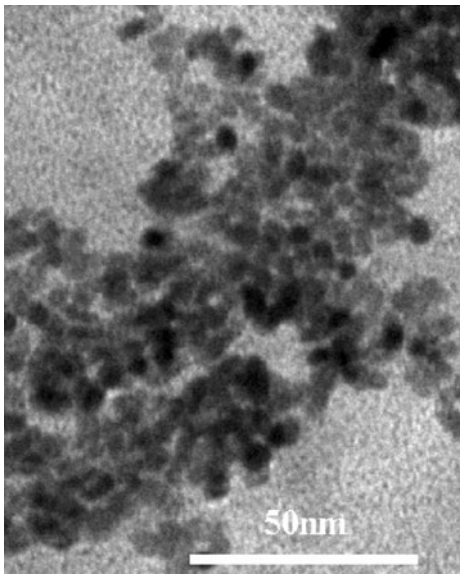


**Fig. 1** TEM image of CS–PDDA–PB nanoparticles

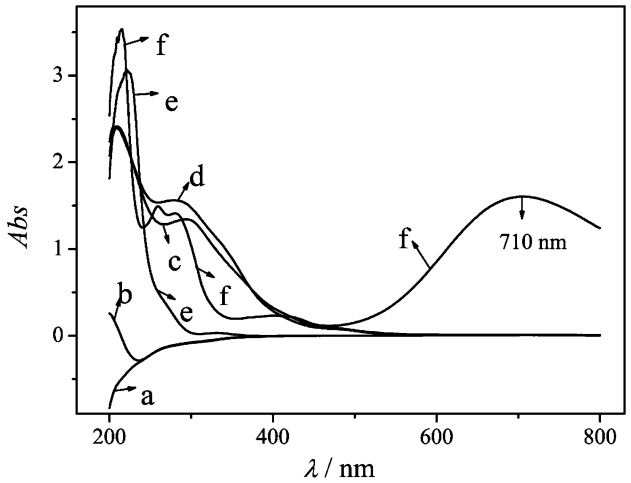


**Fig. 2** UV–vis absorption spectra of (**a**) PDDA, (**b**) CS, (**c**) $FeCl_3$, (**d**) mixture of (**a**) and (**c**), (**e**) $K_4[Fe(CN)_6]$, and (**f**) CS–PDDA–nano-PB colloidal solutions. The blank solution was doubly distilled water

procedure of the sensor was shown in Scheme 1. The electrode was stored at 4 °C when not in use.

## Results and discussion

### UV–vis absorption spectra and TEM characterizations of CS–PDDA–nano-PB

Morphologies of CS–PDDA–PB nanoparticles were characterized by TEM. Figure 1 gives the image of CS–PDDA–PB nanoparticles and the mean size of them was about 7.5 nm. The surface of the CS–PDDA–PB nanoparticles was not smooth. Maybe the PB nanoparticles are packed by CS and PDDA.

The UV–vis absorption spectra of PDDA, CS, $FeCl_3$, mixture of $FeCl_3$ and PDDA, $K_4[Fe(CN)_6]$, and CS–PDDA–nano-PB colloids solutions are shown in Fig. 2. It can be seen from Fig. 2 that alone PDDA or CS solution did not show an absorption peak (curves a and b in Fig. 2). $FeCl_3$ solution had two absorption peaks around 210 and 295 nm (curve c in Fig. 2). But after $FeCl_3$ solution and PDDA were mixed, the second absorption peak shifted to 280 nm, and the absorbance increased a little (curve d in Fig. 2). The maximum absorbance of $K_4[Fe(CN)_6]$ solution appeared approximately at 221 nm (curve e in Fig. 2). When the $K_4[Fe(CN)_6]$ solution was slowly dropped into the mixed solution (containing $FeCl_3$, CS, and 0.4% PDDA), the color of solution was changed to dark blue gradually and a new absorption peak appeared at 710 nm (curve f in Fig. 2), illustrating the characteristic adsorption of CS–PDDA–nano-PB colloid [24, 26].

### Electrochemical characteristics of the self-assembled electrode

Figure 3 shows the CVs of the modified electrode in different assembled steps in the potential range from −0.2 to 0.6 V in 0.02 M PBS (pH 6.0). There was no electrochemical signal at the bare GC electrode in the interesting potential range (curve a). But after the CS–PDDA–PB nanoparticles were cast on the electrode surface, the CV of the GC/CS–PDDA–nano-PB electrode gives a pair of well-defined redox peaks (curve b). When gold nanoparticles were assembled onto the electrode through binding interaction between gold nanoparticles and amino groups of CS and electrostatic interaction between oppositely charged gold nanoparticles and PDDA, an increase in peak current was observed (curve c). The reason is that nanometer-sized gold colloids play an important role similar to an electron-conducting tunnel, which makes it easier for the electron

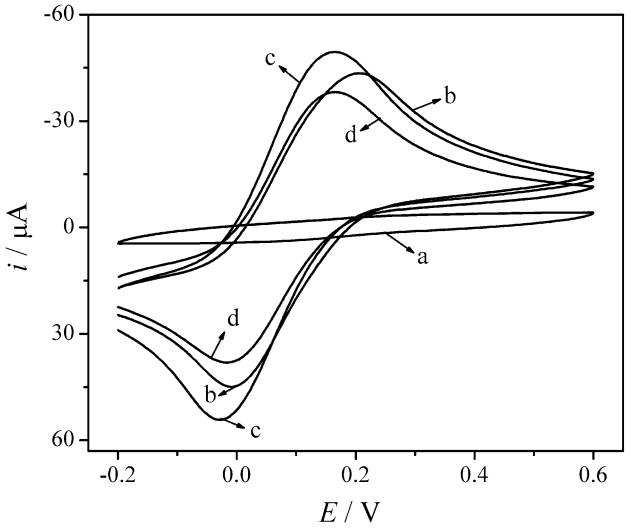


**Fig. 3** CVs of the modified electrode at different assembled stages in 0.02 M PBS (pH 6.0) for (**a**) bare GC, (**b**) GC/CS–PDDA–nano-PB, (**c**) GC/CS-PDDA-nano-PB/nano-Au, and (**d**) GC/CS–PDDA-nano-PB/nano-Au/MPBA. Scan rate: 100 mV/s

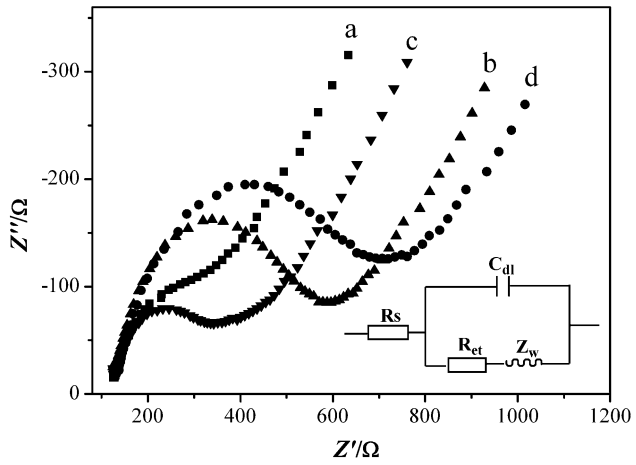


**Fig. 4** EIS of the electrodes at different assembled stages in 5 mM $[Fe(CN)_6]^{3-/4-}$ containing 0.1 M KCl. **a** Bare GC, **b** GC/CS–PDDA–nano-PB, **c** GC/CS-PDDA-nano-PB/nano-Au, **d** GC/CS–PDDA–nano-PB/nano-Au/MPBA. The frequency range is between 0.05 and $10^5$ Hz at the formal potential of 0.22 V. The *inset* shows the equivalent circuit used to model impedance data

transfer. After 4-mercaptophenylboronic acid (MPBA) was assembled onto the electrode via a sulfur-Au bond, the peak current decreased obviously (curve d), suggesting that MPBA monolayer was not beneficial to the electron transfer.

The assembly process of the modified electrode was also monitored by EIS since it is an effective method to probe the interface properties of surface-modified electrodes. Figure 4 shows the EIS results for different electrodes in a 5.0 mM $[Fe(CN)_6]^{4-/3-}$ + 0.1 M KCl solution as a redox probe. It can be seen from Fig. 4 that compared with the bare GC electrode (curve a), an obvious semicircle was observed at the CS–PDDA–nano-PB modified GC electrode with a diameter of 338.3 Ω (curve b). When gold nanoparticles were assembled onto the GC/CS–PDDA–nano-PB electrode, the $R_{et}$ decreased to 175.3 Ω (curve c), which contributed to the good conductive properties of gold nanoparticles. In comparison with curve c of Fig. 4, the semicircle increased obviously after MPBA was assembled onto the electrode with a diameter about 381.7 Ω (Fig. 4, curve d), indicting that the MPBA monolayer hinders the charge transfer. On the basis of the EIS results, we can conclude that MPBA was successfully assembled onto the electrode surface.

Self-assembled time is an important factor which would influence the electrochemical response of the assembled monolayer. Figure 5a shows the relationship between assembling time of nano-Au and current response of the GC/CS–PDDA–nano-PB/nano-Au electrode. It can be seen from Fig. 5a that the current response of the GC/CS–PDDA-nano-PB/nano-Au electrode increased with an increase in assembling time of nano-Au and reached the maximum after about 9 h assembling time. Therefore, 9 h was chosen as the suitable assembling time for nano-Au. In addition, the optimum of assembling time for MPBA was investigated and the result is shown in Fig. 5b. As can be seen, the suitable assembling time for MPBA was about 10 h. Thus, in the further study we chose the optimum assembling time to obtain a high analytical sensitivity.

The CVs of the self-assembled electrode at different scan rates are shown in Fig. 6. It can be seen from Fig. 6 that both anodic and cathodic peak currents increased linearly with the square root of scan rate between 50 and 700 mV/s (the inset of Fig. 6) with the correlation coefficients of 0.9907 and 0.9995, respectively, indicating a diffusion-controlled redox process.

From the linear relationship between the peak current and the square root of scan rate, the surface area of the electrode could be determined. When the electrode was modified with nanoparticles, the surface area of the electrode was usually larger than the area of geometry, because of the high surface area and strong adsorption ability of nanoparticles. In this paper, the surface area of the self-assembled electrode was calculated according to the following equation:

$$i_p = 2.69 \times 10^5 A n^{3/2} D^{1/2} C v^{1/2} \quad (1)$$

where $A$ is the surface area of the electrode, $n$ the electron transfer number, $D$ the diffusion coefficient, and $C$ the bulk concentration. From the slope of $i_p$ versus $v^{1/2}$, $A$ can be obtained if the parameters of $D$, $n$, and $C$ are known. In this experiment, CVs of the bare GC electrode in a 2.0 mM $[Fe(CN)_6]^{4-/3-}$ solution at different scan rates are presented in Fig. 7. Inset of Fig. 7 shows the linear relationship

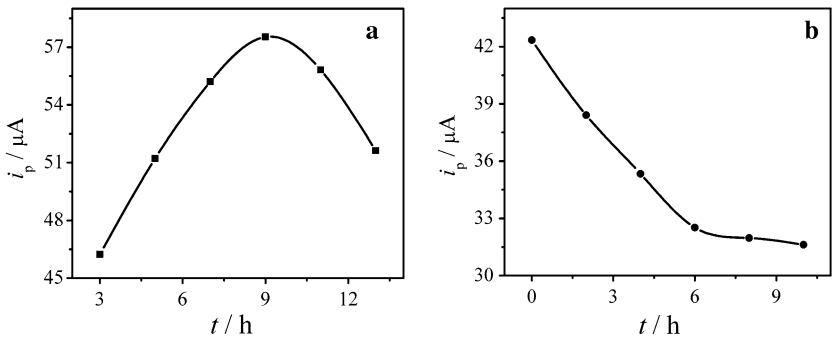


**Fig. 5** Influence of the assembling time of nano-Au (**a**) and MPBA (**b**) on the electrochemical response of different modified processes. Scan rate: 100 mV/s

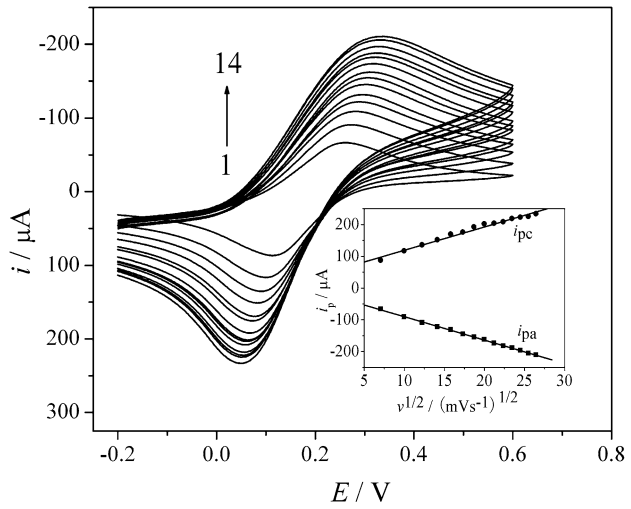


**Fig. 6** CVs of the self-assembled electrode in a 5.0 mM $[Fe(CN)_6]^{3-/4-}$ solution containing 0.1 M KCl at the scan rate (from 1 to 14, mV/s): 50, 100, 150, 200, 250, 300, 350, 400, 450, 500, 550, 600, 650, and 700. The *inset* shows the linear relationship between the peak current and the square root of scan rate

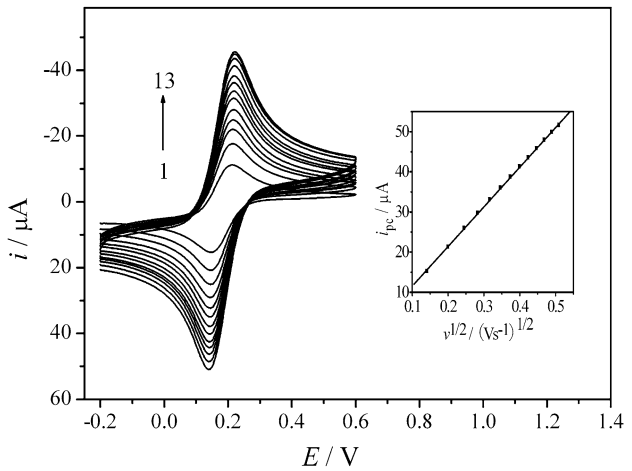


**Fig. 7** CVs of the bare GC electrode in a 2.0 mM $[Fe(CN)_6]^{3-/4-}$ solution containing 0.1 M KCl at the scan rate (from 1 to 13, mV/s): 20, 40, 60, 80, 100, 120, 140, 160, 180, 200, 220, 240 and 260. The *inset* shows the linear relationship between $i_{pc}$ and $v^{1/2}$

between cathodic peak current and the square root of scan rate, and the slope is $9.86 \times 10^{-5}$ $A/(Vs^{-1})^{1/2}$. Thus, the diffusion coefficient was calculated to be $6.72 \times 10^{-6}$ $cm^2/s$ at 25 °C. Then the self-assembled electrode was used as the working electrode also in a 2.0 mM $[Fe(CN)_6]^{4-/3-}$ solution to record the CVs at different scan rates and then from the slope of the plot between $i_{pc}$ and $v^{1/2}$, $A$ was calculated as 0.23 $cm^2$, which was three times larger than the area of geometry (0.07 $cm^2$).

Boronic acids are known to assume an anionic form in alkaline solutions for the addition of the $OH^-$ ion to the boron atom. Therefore, the surface density of the anionic charges on the MPBA film-modified electrode would be a function of pH of the solution in which the electrode is immersed. Thus, the voltammetric behavior of the self-assembled electrode toward anionic species in solution may depend on pH. In this experiment, CVs of the $[Fe(CN)_6]^{4-/3-}$ ion towards the self-assembled electrode in different pH values were recorded as shown in Fig. 8. The $i_p$ was obtained and plotted as a function of

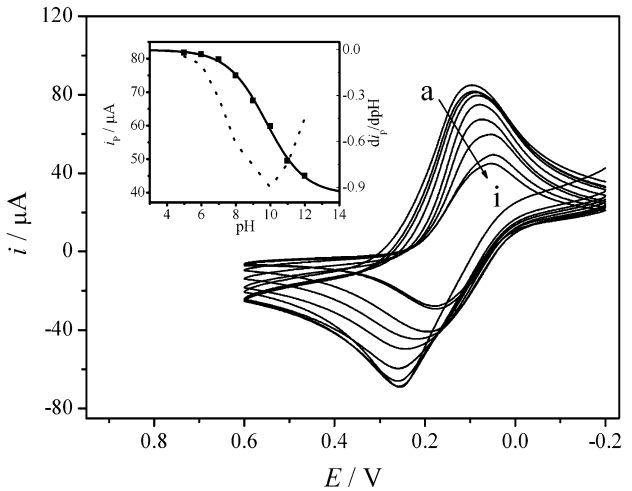


**Fig. 8** CVs of the self-assembled electrode in different PBS containing 0.1 M KCl in the presence of 5 mM $[Fe(CN)_6]^{3-/4-}$. pH (from **a** to **i**): 4.0, 5.0, 6.0, 7.0, 8.0, 9.0, 10.0, 11.0 and 12.0. Scan rate: 100 mV/s. The *inset* shows peak current titration curve for the surface of self-assembled electrode. *Filled square* experimental data; *solid line* titration curve; *dotted line* differential curve of experimental data

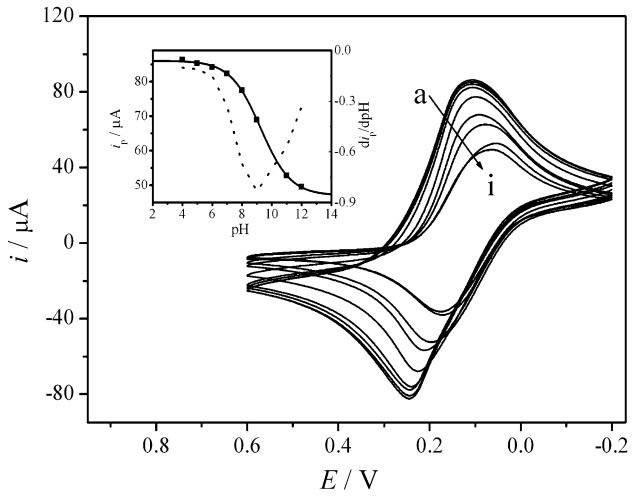


**Fig. 9** CVs of the self-assembled electrode in the presence of sugar in different pH PBS containing 0.1 M KCl in the presence of 5 mM $[Fe(CN)_6]^{3-/4-}$. Take mannose as an example and its concentration was 10.0 mM. pH (from **a** to **i**): 4.0, 5.0, 6.0, 7.0, 8.0, 9.0, 10.0, 11.0 and 12.0. Scan rate: 100 mV/s. The *inset* shows peak current titration curve. *Filled square* experimental data; *solid line* titration curve; *dotted line* differential curve of experimental data

solution pH to obtain the titration curve as shown in the inset of Fig. 8. The surface $pK_a$ of self-assembled electrode can be obtained according to the following equation [32, 34]:

$$pK_a = \text{pH} + \log[(i_{AH} - i)/(i - i_{A-})] \quad (2)$$

where $i_{AH}$ and $i_{A-}$ are the peak currents observed for the neutral and fully negatively charged monolayer-modified electrodes, and $i$ is the peak current in the CV recorded at a given pH where the current is changing the most. The solid line in the inset of Fig. 8 is the titration curve, and the dotted line is the differential curve of experimental data. The differential curve showed that the lowest point was the given pH where the change of peak current was the largest. So according to Eq. 2, the surface $pK_a$ was calculated to be 10.13 for GC/CS–PDDA–nano-PB/Nano-Au/MPBA.

## Electrochemical behavior of the self-assembled electrode towards sugars

The anionic form of boronic acid or derivatives in alkaline solutions bind the 1, 2- or 1, 3-diol of sugars to form anionic boronate esters, which would limit the access of $[Fe(CN)_6]^{3-/4-}$ to the electrode surface due to the electrostatic repulsion. Therefore, pH condition is an important parameter for sugar detection. Figure 9 shows the CVs of the $[Fe(CN)_6]^{3-/4-}$ ion towards the self-assembled electrode in the presence of mannose in different pH values. The solid line in the inset of Fig. 9 is the titration curve, and the dotted line is the differential curve of experimental data. From Eq. 2 mentioned above, the $pK_{a\text{-diol}}$ of mannose was obtained to be 8.88. Similarly, the $pK_{a\text{-diol}}$ values for glucose and fructose were calculated to be 8.90 and 7.87, respectively. The optimal pH for detecting sugars should be between the $pK_a$ values of the boronic acid and diol, which can be obtained from the following equation [35]:

$$\text{pH}_{\text{optimal}} = (pK_{a,\,\text{boronicacid}} + pK_{a,\,\text{diol}})/2 \quad (3)$$

Therefore, the optimal pHs for binding of mannose, glucose, and fructose with immobilized MPBA can be predicted from Eq. 3 to be 9.5, 9.52 and 9.0, respectively. The optimal pHs were selected as the investigation in the following experiment.

Under the optimum conditions given above, quantitative detection of sugars at the GC/CS–PDDA-nano-PB/nano-Au/MPBA electrode was investigated. The peak currents $\Delta i_p$ ($\Delta i_p = i_{po} - i_{pc}$, $i_{po}$: the reduction peak current in the absence of sugars; $i_{pc}$: the reduction peak current in the presence of sugars) were measured and then plotted against the concentration of different sugars. The linear response equations and the detection limits for glucose, mannose, and fructose are presented in Table 1.

Regeneration and stability of biosensors are very important in their application and development. In this paper, the assembled electrode could be regenerated by simply immersing it in a 0.1 M PBS (pH 6.0) for 15 min followed by washing with water, and the regenerated electrode could be used repeatedly for sugar detection. In

**Table 1** Analytical parameters for the three sugars on the modified electrode

| Sugar | Linear range (mM) | Regression equation $C$ (mM); $\Delta i_p$ (μA) | Correlation coefficient | Detection limit (mM) |
|---|---|---|---|---|
| D-Glucose | 0.1–1.0 | $\Delta i_p = 1.90 + 0.88\ \log C$ | 0.9994 | 0.026 |
| | 1.0–100 | $\Delta i_p = 1.91 + 0.22\ \log C$ | 0.9977 | |
| D-Mannose | 0.1–0.55 | $\Delta i_p = 1.56 + 0.71\ \log C$ | 0.9997 | 0.059 |
| | 0.55–120 | $\Delta i_p = 1.40 + 0.06\ \log C$ | 0.9960 | |
| D-Fructose | 0.1–0.5 | $\Delta i_p = 2.33 + 0.94\ \log C$ | 0.9999 | 0.022 |
| | 0.5–100 | $\Delta i_p = 2.12 + 0.26\ \log C$ | 0.9985 | |

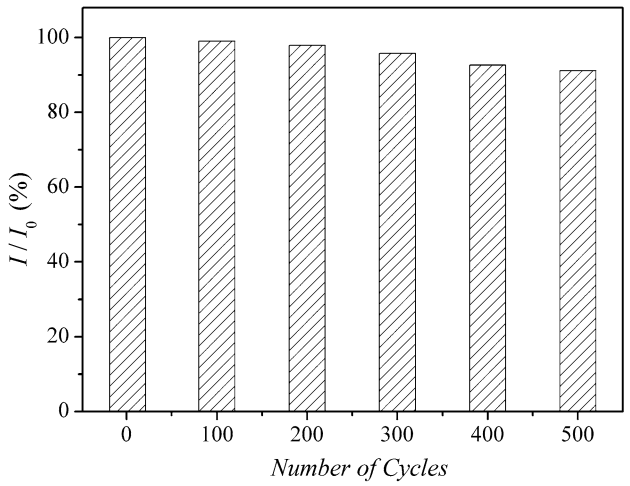


**Fig. 10** Relationship between the reduction peak current and sweeping cycle in 0.02 M PBS (pH 6.0). Scan rate: 100 mV/s

addition, the experimental results about the stability of the self-assembled electrode are shown in Fig. 10. When the electrode was cyclically swept for 500 cycles, the reduction peak current remained 91.2% of the initial response, showing its good stability.

## Conclusion

A new biosensor based on immobilization of MPBA on the surface of GC/CS–PDDA-nano-PB/nano-Au electrode was fabricated. In this work, the PB nanoparticles synthesized with CS and PDDA as stabilization agents can be immobilized on the surface of GC electrode and are conducive to assembling nano-Au and MPBA to obtain the self-assembled electrode. This electrode was characterized and has been proved to be sensitive for the determination of sugars.

**Acknowledgments** The authors gratefully acknowledge the support by the National Natural Science Foundation of China (no. 20575054), China (NSFC)-Korea (KOSEF) Joint Research Project (no. 20811140329) and the Municipal Science Foundation of Chongqing City (no. CSTC-2008BB4012, CSTC-2008BB4013).

## References

1. Dequaire M, Degrand C, Limoges B (2000) An electrochemical metalloimmunoassay based on a colloidal gold label. Anal Chem 72:5521–5528
2. Gish DA, Nsiah F, McDermott MT, Brett MJ (2007) Localized surface plasmon resonance biosensor using silver nanostructures fabricated by glancing angle deposition. Anal Chem 79:4228–4232
3. Hrapovic S, Liu YL, Male KB, Luong JHT (2004) Electrochemical biosensing platforms using platinum nanoparticles and carbon nanotubes. Anal Chem 76:1083–1088
4. Streeter I, Baron R, Compton RG (2007) Voltammetry at nanoparticle and microparticle modified electrodes: theory and experiment. J Phys Chem C 111:17008–17014
5. Xian YZ, Hu Y, Liu F, Xian Y, Feng LJ, Jin LT (2007) Template synthesis of highly ordered Prussian blue array and its application to the glucose biosensing. Biosens Bioelectron 22:2827–2833
6. Itaya K, Uchida I, Neff VD (1986) Electrochemistry of polynuclear transition metal cyanides: Prussian blue and its analogues. Acc Chem Res 19:162–168
7. Kaneko M, Hara S, Yamada A (1985) A photoresponsive graphite electrode coated with Prussian blue. J Electroanal Chem 194:165–168
8. Kulesza PJ, Miecznikowski K, Chojak M, Malik MA, Zamponi S, Marassi R (2001) Electrochromic features of hybrid films composed of polyaniline and metal hexacyanoferrate. Electrochim Acta 46:4371–4378
9. DeLongchamp DM, Hammond PT (2004) Multiple-color electrochromism from layer-by-layer assembled polyaniline/Prussian blue nanocomposite thin films. Chem Mater 16:4799–4805
10. Einaga Y, Sato O, Iyoda T, Fujishima A, Hashimoto K (1999) Photofunctional vesicles containing Prussian blue and azobenzene. J Am Chem Soc 121:3745–3750
11. Itaya K, Shoji N, Uchida I (1984) Catalysis of the reduction of molecular oxygen to water at Prussian blue modified electrodes. J Am Chem Soc 106:3423–3429
12. Karyakin AA, Gitelmacher OV, Karyakina EE (1994) A high-sensitive glucose amperometric biosensor based on Prussian blue modified electrodes. Anal Lett 27:2861–2869
13. Karyakin AA (2001) Prussian blue and its analogues: electrochemistry and analytical applications. Electroanalysis 13:813–819
14. Chen LC, Ho KC (2008) Multimode opto-electrochemical detection of cysteine based on an electrochromic Prussian blue electrode. Sensor Actuat B 130:418–424
15. Karyakin AA, Gitelmacher OV, Karyakina EE (1995) Prussian blue-based first-generation biosensor: a sensitive amperometric electrode for glucose. Anal Chem 67:2419–2423
16. Zhao H, Yuan Y, Adeloju S, Wallace GG (2002) Study on the formation of the Prussian blue films on the polypyrrole surface as a potential mediator system for biosensing applications. Anal Chim Acta 472:113–121
17. Ho KC, Chen CY, Hsu HC, Chen LC, Shiesh SC, Lin XZ (2004) Amperometric detection of morphine at a Prussian blue-modified indium tin oxide electrode. Biosens Bioelectron 20:3–8
18. Gorton L (1995) Carbon paste electrodes modified with enzymes, tissues, and cells. Electroanalysis 7:23–45
19. Ricci F, Palleschi G (2005) Sensor and biosensor preparation, optimization and applications of Prussian blue modified electrodes. Biosens Bioelectron 21:389–407
20. Uemura T, Ohba M, Kitagawa S (2004) Size and surface effects of Prussian blue nanoparticles protected by organic polymers. Inorg Chem 43:7339–7345
21. Li ZH, Zhang JL, Mu TC, Du JM, Liu ZM, Han BX, Chen J (2004) Preparation of poly-vinylpyrrolidone protected Prussian blue nanocomposites in microemulsion. J Colloids Surf A 243:63–66
22. Zhang Q, Zhang L, Li JH (2008) Fabrication and electrochemical study of monodisperse and size controlled Prussian blue nanoparticles protected by biocompatible polymer. Electrochim Acta 53:3050–3055
23. Zhao W, Xu JJ, Shi CG, Chen HY (2005) Multilayer membranes via layer-by-layer deposition of organic polymer protected Prussian blue nanoparticles and glucose oxidase for glucose biosensing. Langmuir 21:9630–9634
24. Wang L, Guo SJ, Hu XG, Dong SJ (2008) Layer-by-layer assembly of carbon nanotubes and Prussian blue nanoparticles: a

potential tool for biosensing devices. J Colloids Surf A 317:394–399
25. Hornok V, Dékány I (2007) Synthesis and stabilization of Prussian blue nanoparticles and application for sensors. J Colloid Interface Sci 309:176–182
26. Chen SH, Yuan R, Chai YQ, Xu Y, Min LG, Li N (2008) A new antibody immobilization technique based on organic polymers protected Prussian blue nanoparticles and gold colloidal nanoparticles for amperometric immunosensors. Sensor Actuat B 135:236–244
27. Dong SQ, Zhang S, Cheng X, He PG, Wang QJ, Fang YZ (2007) Simultaneous determination of sugars and ascorbic acid by capillary zone electrophoresis with amperometric detection at a carbon paste electrode modified with polyethylene glycol and $Cu_2O$. J Chromatogr A 1161:327–333
28. Lv Y, Zhang ZJ, Chen FN (2003) Chemiluminescence microfluidic system sensor on a chip for determination of glucose in human serum with immobilized reagents. Talanta 59:571–576
29. Bhandari P, Kumar N, Singh B, Kaul VK (2008) Simultaneous determination of sugars and picrosides in *Picrorhiza* species using ultrasonic extraction and high-performance liquid chromatography with evaporative light scattering detection. J Chromatogr A 1194:257–261
30. Chen G, Zhang LY, Wu XL, Ye JN (2005) Determination of mannitol and three sugars in *Ligustrum lucidum* Ait. by capillary electrophoresis with electrochemical detection. Anal Chim Acta 530:15–21
31. Zuo SH, Teng YJ, Yuan HH, Lan MB (2008) Direct electrochemistry of glucose oxidase on screen-printed electrodes through one-step enzyme immobilization process with silica sol–gel/polyvinyl alcohol hybrid film. Sen Actuators B Chem 133:555–560
32. Pribyl J, Skladal P (2006) Development of a combined setup for simultaneous detection of total and glycated haemoglobin content in blood samples. Biosens Bioelectron 21:1952–1959
33. Frens G (1973) Controlled nucleation for the regulation of the particle size in mono-disperse gold suspensions. Nat Phys Sci 241:20–22
34. Zhao JW, Luo LQ, Yang XR, Wang EK, Dong SJ (1999) Determination of surface p$K_a$ of SAM using an electrochemical titration method. Electroanalysis 11:1108–1111
35. Yan J, Springsteen G, Deeter S, Wang BH (2004) The relationship among p$K_a$, pH, and binding constants in the interactions between boronic acids and diols-it is not as simple as it appears. Tetrahedron 60:11205–11209